

# Characterization of a Thin Film Phantom for contrast and resolution measurements

Stephen A. McAleavey<sup>\*a</sup>, Robert G. Naum<sup>b</sup>, Kevin J. Parker<sup>a</sup>

<sup>a</sup>University of Rochester, Dept. of Electrical Engineering, Rochester, NY 14627

<sup>b</sup>Applied Image, Inc., Rochester, NY 14609

## ABSTRACT

This paper describes the characterization of a unique thin-film ultrasound phantom. The phantom consists of a film with controllable acoustic properties immersed in an ultrasonically transparent material. The placement of scattering sites on the film creates an image when scanned with a clinical instrument.

The backscatter from a halftoned region as a function of halftone density is presented for white and blue noise halftoning. Simulations and measurements were found to be in agreement with a theory for scattering from a dense concentration of point targets. The results indicate a maximum contrast of 19dB may be achieved with the material selected, and contrast may be controlled over a 10dB range.

A suitable character set for testing the MTF of a clinical instrument has been selected. A study using simulated ultrasound images is presented demonstrating the suitability of the character set and suggesting future modifications.

The resolution of a medical ultrasound imaging system was determined using a wire phantom and thin-film techniques. The results were found to be consistent with one another, with the thin-film phantom indicating a lower resolution due to its lower overall contrast. Reduced contrast in the thin-film lead to a further reduction in the measured resolution.

**Keywords:** phantom, ultrasound, Thin Film Phantom, image quality, halftoning

## 1. INTRODUCTION

With the development of teleradiology comes a need to ensure the fidelity of the full teleradiographic imaging chain. An inexpensive, easy to use phantom would facilitate this process by allowing a radiologist to evaluate the quality of an image of a known target. The Thin Film Phantom lends itself to this application. Phillips and Parker<sup>1</sup> give the principle of operation of the Thin Film Phantom in detail in an earlier paper. Briefly, the concept is to create a thin film or membrane with carefully placed scattering sites on or within the film. The film is then immersed in a fluid to support the propagation of ultrasound. The film is chosen to have a minimal effect on the propagation of the acoustic wave, save for the scattering sites which give rise to an image when the film is aligned with the scan plane of an ultrasound instrument.

### 1.1 Vesicular Film

The phantoms in this study were created using Vesicular<sup>TM</sup> microfiche film. The film is a layered thermoplastic with an ultraviolet-sensitive middle layer. This layer is a mixture of plastic and diazo salts. These salts break down in the presence of ultraviolet light, generating nitrogen gas in the process. Exposing the film to a UV image generates a latent image in the film of decomposed salts. Heating the film after exposure softens the film, allowing the entrapped gas to expand into bubbles. These bubbles are on the order of 1 $\mu$ m in diameter. The optical effect is to create a dense blue cast in the exposed areas. Unexposed areas retain the transparency of the substrate. Subsequent processing steps desensitize the remaining diazo salts and permanently fix the image.

---

\* Correspondence: Email: mcaleave@ece.rochester.edu; Telephone: 716 275 3755

The acoustic properties of the film are also altered by exposure. One might expect that the individual nitrogen filled bubbles in the film would act as scatterers. However, exposed areas that are large relative to the ultrasound wavelength used to probe them do not behave as strong scattering regions. Rather, the edges of the exposed region are visualized, while the interior appears dark. This leads to the conclusion that the generation of bubbles in the film alters the acoustic properties of the exposed area in a uniform way, such that an exposed region appears as a different material than the substrate.

The diffuse scatter seen in ultrasonic investigations of tissue is due to small variations in the acoustic properties of the tissue on a scale much smaller than a wavelength. This suggests that scattering regions may be generated in the Vesicular film by halftoning the region with a screen pitch much smaller than a wavelength. The small variations in acoustic properties thus introduced will give rise to scattering of the incident ultrasound.

## 2. HALFTONE EVALUATION

### 2.1. Simulations and theoretical model

Simulations were conducted to determine the best halftone screen for contrast control. Regular (deterministic) screens were ruled out because of the frequency-selective nature of the scattering from a periodic array. Two pseudo-random screens were considered: the Blue Noise Mask<sup>2</sup> and white noise. Simulations of the backscatter intensity from regions of varying halftone density were carried out for each mask. The simulation results appear in Figure 1.

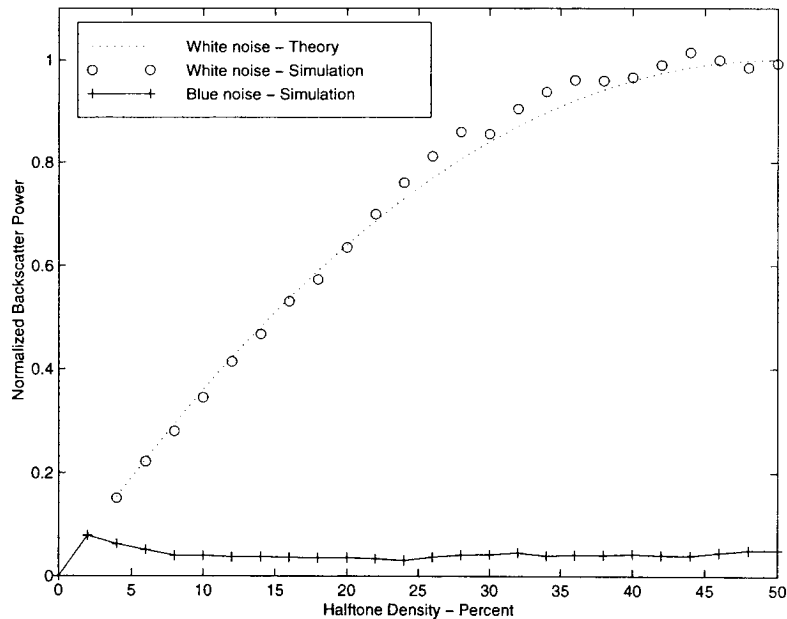


Figure 1. Backscatter power as a function of halftone density for white and blue noise screens.

Mo and Cobbold<sup>3</sup> explain these power/density relationships in a paper examining the backscattered signal from whole blood. They demonstrate that the backscattered power from a dense collection of point scatterers is proportional to the average variance in scatterer concentration in an insonified region. The halftoning of a plane with white noise can be considered the result of a Bernoulli random process. Each point on the halftone grid is 'on' or 'off' given the outcome of each Bernoulli trial. If the number of grid points  $N$  is large within a subresolvable region of the halftone, the probability that  $n$  points out of the  $N$  in the region are filled can be approximated by the Gaussian distribution

$$P_N(n) \approx \frac{1}{\sqrt{2\pi Nx(1-x)}} e^{-\frac{(n-Nx)^2}{2Nx(1-x)}} \quad (1)$$

which has a variance of  $Nx(1-x)$ . This together with the proportionality determined by Mo and Cobbold leads to an expression for the backscattered power as a function of halftone density for white noise

$$B(x) = 4Ax(1 - x) \quad (2)$$

where  $B(x)$  is the backscatter as a function of halftone density  $x$ , with  $0 \leq x \leq 1$ .  $A$  is a constant determined by the average scattering strength of a 50% halftone pattern.

The Blue Noise Mask displays a relatively flat backscatter versus halftone density curve for between 5-50%. In contrast to white noise, blue noise is carefully designed to fill a region as uniformly as possible, without large-scale variations. Therefore, once the halftone density becomes great enough for speckle to develop from the interaction of point scatterers, the very nearly constant variance in scatterer density prevents any further increase in backscatter, as is seen in Figure 1.

The maximum dynamic range of the halftoned phantom is limited by failure of very sparse halftones to develop speckle. At very low halftone densities, below approximately 2%, the space between individual points becomes so great that speckle is not developed. Instead, the Point Spread Function (PSF) of the imaging system is generated at the scattering sites. The separation between the scatterers prevents the development of coherent scatter and speckle. This lets us set 2% as a lower limit for halftone density for controlled foreground / background (lesion / tissue) contrast phantoms. Of course, for high contrast measurements, as in a conventional wire phantom, the background density may be set to zero. Referring to equation 2, this limit implies a dynamic range of 10dB for the phantom.

## 2.2 Experimental measurements

To verify the simulations, a set of four films was generated. The halftones were generated using a MATLAB script whose output was a TIFF file used to create a mask for exposing the Vesicular film. A sample is illustrated in Figure 2. The exposed area measures 5.1x5.1 cm. The reference patch was halftoned at 50%, while the test patches were halftoned at 0, 5, 10, and 20%, one density per film. The purpose of the 0% test film was to establish a noise floor due to any intrinsic film scatter. At the final print size, the halftone pitch was 600dpi. This corresponds to a dot size of 42 $\mu$ m. At 3MHz this is less than 1/10 of a wavelength. Thus, each printed dot behaves as a Rayleigh scatterer.

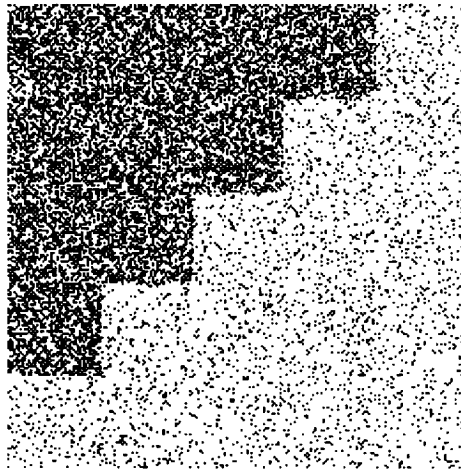


Figure 2. Test patch for determining halftone/backscatter relationship, with the 50% reference patch at upper left and a 5% test patch at lower right,

The films were immersed in an anechoic tank filled with degassed, demineralized water. The walls of the tank were covered with soft rubber, and the base with a stack of wedge-cut rubber slabs to prevent reverberations. The films were held in tension by their corners to ensure they remained flat. The films were allowed to sit several hours under water to allow any air bubbles on the surface of the film to be absorbed into the water, as well as to allow any impurities in the water to settle out. The film was scanned with a HP Sonos 100 scanner using a 2.5MHz mechanically steered transducer. The scanner has been

modified to provide RF and Start-of-A-line (LINE) signals at BNC connectors on the instrument. The RF and LINE signals were fed to a digitizing oscilloscope (LeCroy). The transducer scan plane was aligned with the film using the sector scan mode. The scanner was then switched to M-mode. This allowed single A-lines to be collected by the oscilloscope along any line of the scan plane. At least four lines were collected each from the test and reference areas of the film. The data was captured and transferred to a PC. The average RMS value of the test and reference patches was calculated. The ratio of the test/reference average RMS values was plotted against halftone density. The result appears in Figure 3.

We found that the 0% halftone produces a  $-19\text{dB}$  signal relative to the 50% halftone section, due to inherent scattering properties of the substrate. In comparison, the wire phantom has a wire / background contrast of  $>23\text{dB}$ . The 5% screen yielded a  $10\text{dB}$  contrast with the 50% reference patch.

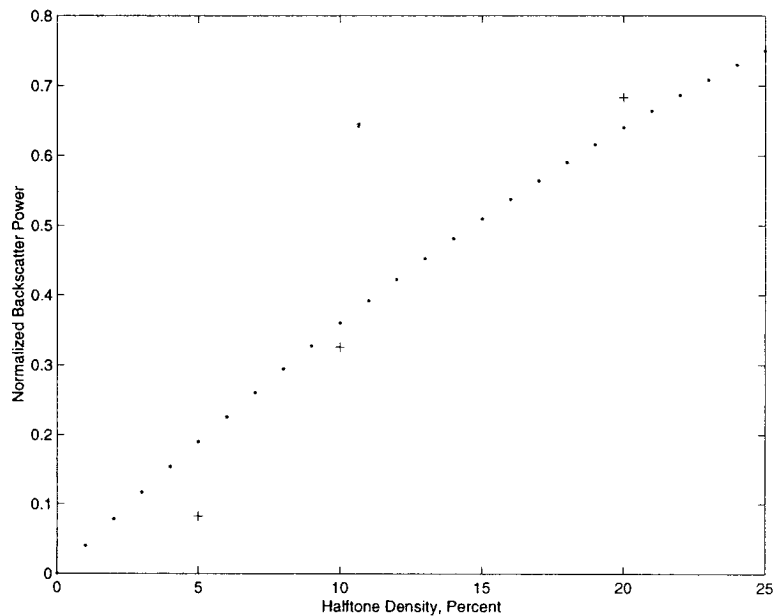


Figure 3. The measured backscattered power from halftoned film (crosses) agrees with the theoretical model.

### 3. CHARACTER SET EVALUATION

To evaluate system MTF we propose to use a set of block characters of varying size, similar to a doctor's eye chart. Such a set of characters is incorporated in the RIT Resolution Test object<sup>4</sup>. The five characters chosen (2, 3, 5, 8, E) are constructed with a  $5 \times 5$  square matrix. The characters are scaled over a range suitable to determining the resolution of the system under test. These characters were studied by Donaldson and Gough<sup>5</sup> and found to be equally recognizable regardless of size.

To check the suitability of this character set for the purposes of the thin film phantom, a small study was carried out. The point spread function (PSF) of a Quantum QAD-1 medical ultrasound scanner with a 3MHz linear array was estimated with a wire phantom. A set of 250 halftone characters from the RIT set was generated. The set was divided into 5 groups of 50, with character heights of 11, 10, 9, 8 and 7 mm. Each size group contained 10 instances of each character. Ultrasound scanning of the characters with the QAD-1 scanner was simulated using the theory described by Macovski<sup>6</sup>. The pulse center frequency was 3MHz and the (Gaussian) envelope was given FWHM dimensions of 1.1mm (axial) by 2.2 mm (lateral) as estimated from the wire phantom. A sample of the halftone characters and the simulated output is given in Figure 4.

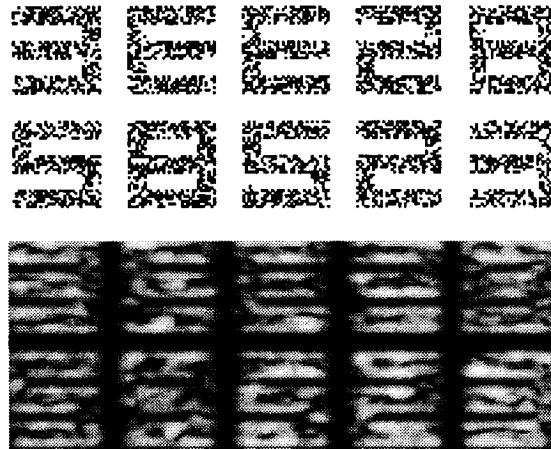


Figure 4. Halftone characters (top) and simulated ultrasound scan.

The ultrasound images were shown to nine observers, one observer at a time, on a CRT display. Each observer was asked to read the characters they saw. The character was categorized as 'blurred' if it was unintelligible to the observer. The sequence of images was randomized in size for each observer. A co-occurrence matrix of the input/output response for each character size and observer was generated. Elements  $M_{ij}$  of the matrix gives the number of times character  $i$  was given as a response when character  $j$  was shown. The matrix would be diagonal if the responses were perfectly correct. The matrices for a given character size were summed over all observers. The results appear in Tables I-IV.

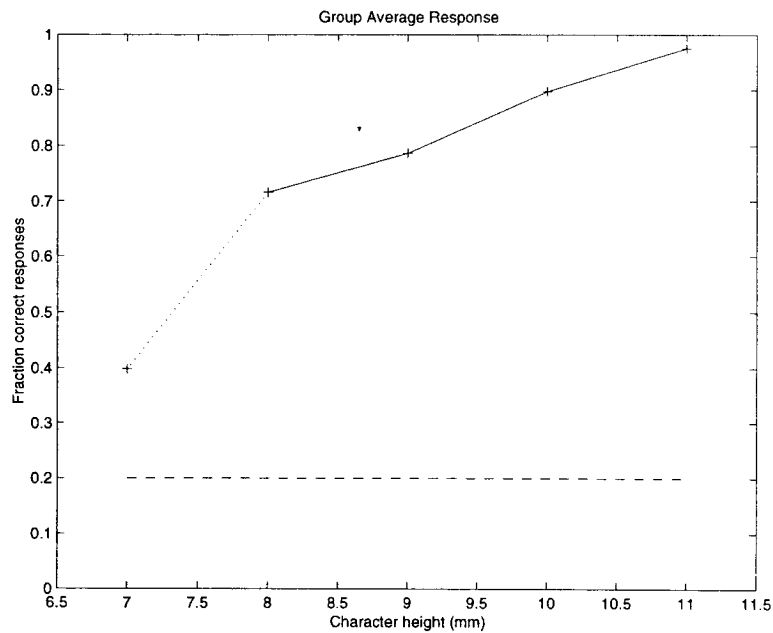


Figure 5. Observer performance drops with decreasing character size, approaching chance probability (dashed line) at a character height of 7mm

The simplest analysis is to determine the fraction of correct responses for a given character size. This is found by dividing the trace of the matrix by the sum of all its elements. The result is shown in Figure 5. As expected, the number of correct responses decreases with the size of the characters. It should be noted that most of the observers said they could not read characters at the 7mm size. The 7mm result is drawn from the responses of the two observers who felt they were able to read the smallest characters. They do about twice as well as chance would predict.

One concern with any test character set is that each character be equally recognizable near the threshold of perception. That is, one would like a set in which each character has an equal probability of being read correctly as they become blurred to the point of imperceptibility by the imaging system. The RIT set was designed for this to be true in optical imaging systems, specifically, for airborne film camera systems. Given the nature of ultrasound image formation, particularly the coherent illumination of the target and resulting speckle, it is possible that the character equivalence will no longer hold. This is suggested in looking at Tables I-IV, where the character '8' appears to produce substantially more false outputs than other characters. To address this issue, a sensitivity/specificity figure of merit was calculated for each character at each size.

The sensitivity to a particular character  $i$  is taken to be

$$Sensitivity(i) = \frac{TP}{TP + FN} = \frac{M_{i,i}}{\sum_k M_{k,i}} \quad (3)$$

while the specificity is given by

$$Specificity(i) = \frac{TN}{TN + FP} = \frac{\sum_{j,k} M_{j,k} \quad j,k \neq i}{\sum_{j,k} M_{j,k} \quad k \neq i} \quad (4)$$

where TP, TN, FP, FN are the numbers of true positive, true negative, false positive and false negative responses. The figure of merit for each character is found by taking the product of the sensitivity and specificity. It is clear from Table V that the character '8' is significantly less recognizable than the others. This may be due to apparent breaks in the sides of the '8' due to speckle, leading to it being interpreted as another character. Indeed, an '8' with any vertical segment missing is equivalent to two other characters with an extra vertical segment. The results suggest that observers are more likely to assume that image blur adds segments rather than deleting them, causing '8' to create false positives for many other characters.

#### 4. RESOLUTION MEASUREMENT

A resolution measurement was carried out using a Thin Film Phantom. A halftone character ramp with heights of 7 to 12 mm in 0.1mm increments was created and printed on Vesicular film. The final print had a halftone pitch of 42 $\mu$ m. The foreground and background densities were 50% and 0% respectively. The pattern used is illustrated in Figure 6. The image was scanned using a setup similar to that described in section 2.2 except that the Quantum QAD-1 scanner with a 3MHz linear array was used to form an image. The target was scanned with the characters in both horizontal (illustrated) and vertical orientations to obtain estimates of the difference in horizontal and vertical resolution. The composite video output of the scanner was captured with a frame grabber. In addition, an image of a wire phantom chirp target, where the spacing between successive wire pairs increases by a constant factor, was captured. In both instances the gain and power controls were set to obtain the best image possible.

The captured images, illustrated in Figures 6 and 7, were shown to a group of ten observers. As in the study described previously, they were shown the five element character set and asked to read the character ramp to the smallest character possible. For the wire target they were asked to give the number of dots visible in the horizontal and vertical chirps.

No observer could read any character smaller than 8mm tall, corresponding to 0.31 cycles/mm. All but two were able to distinguish a 9.5mm tall character, corresponding to 0.26 cycles/mm. They were unable to distinguish two wires separated by 1.5mm (0.67 cycles/mm) but could resolve wires separated by 2.5mm (0.4 cycles/mm). Use of the Thin Film Phantom suggests a lower resolution than is attainable with the wire phantom, but this is probably due to the 4dB difference in contrast between the two.

Table I. Responses for 11mm size characters

		INPUT				
		2	3	5	8	E
OUTPUT	2	89	0	0	1	0
	3	0	89	1	3	2
	5	0	0	89	1	1
	8	0	0	0	85	0
	E	1	1	0	0	87

Table II. Responses for 10mm size characters

		INPUT				
		2	3	5	8	E
OUTPUT	2	84	3	0	15	1
	3	0	83	4	0	0
	5	0	0	84	8	1
	8	3	1	0	66	4
	E	3	1	2	0	84

Table III. Responses for 9mm size characters

		INPUT				
		2	3	5	8	E
OUTPUT	2	73	2	1	9	1
	3	1	70	6	4	2
	5	1	3	70	3	5
	8	6	11	6	56	5
	E	8	0	4	15	73

Table IV. Responses for 8mm size characters

		INPUT				
		2	3	5	8	E
OUTPUT	2	62	9	0	6	4
	3	6	62	11	2	1
	5	2	4	54	14	11
	8	8	4	6	42	2
	E	5	3	6	10	67

Table V. Figure of Merit for characters

		CHARACTER				
		2	3	5	8	E
Size (mm)	11	0.99	0.97	0.98	0.94	0.96
	10	0.88	0.93	0.91	0.73	0.92
	9	0.79	0.78	0.78	0.59	0.78
	8	0.70	0.71	0.63	0.53	0.73

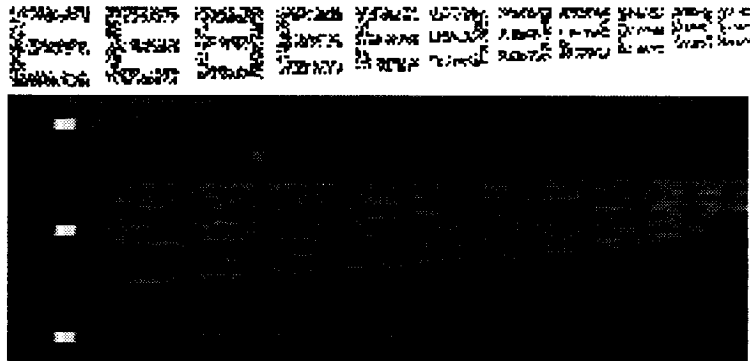


Figure 6. Halftoned character ramp (top) for resolution measurement and 3MHz ultrasound image of the Vesicular film print.

